

RECTIFIER SUBSTATIONS

Electrical supply substations (ESSs) in dc traction systems, supplied by one or more high-voltage ac lines, convert the ac side high-voltage into desired dc side voltage (1). Figure 1 shows the basic scheme of an electrical supply substation, which includes high-voltage three phase lines, high-voltage three phase busbars, conversion units, and positive and negative dc busbars. There are two different ways to correct a substation with supply lines: series connection, when the primary lines are directly connected to the substation busbars and pass through them, and branching connection, when the substation is connected to the primary lines without any sectioning. Figure 2 shows both types of connections. Conversion groups are protected on the ac side by a three-phase switch and are equipped with a three-phase transformer, which steps down the voltage according to the desired voltage magnitude, and a diode bridge rectifier, in the 6-pulse or 12-pulse configuration. Most existing large metrorail plants are equipped with 6-pulse units, but the recent trend is to utilize 12-pulse units (in parallel connection, with or without an intergroup reactor) both in metrorail and railway systems. The 12-pulse option is considered because of its reduced harmonic impact on the supply network, its better utilization of the transformer, its flexibility in control of the voltage regulation characteristic (in terms of voltage drop and short circuit current), and its reduced dc voltage ripple. The 12-pulse series

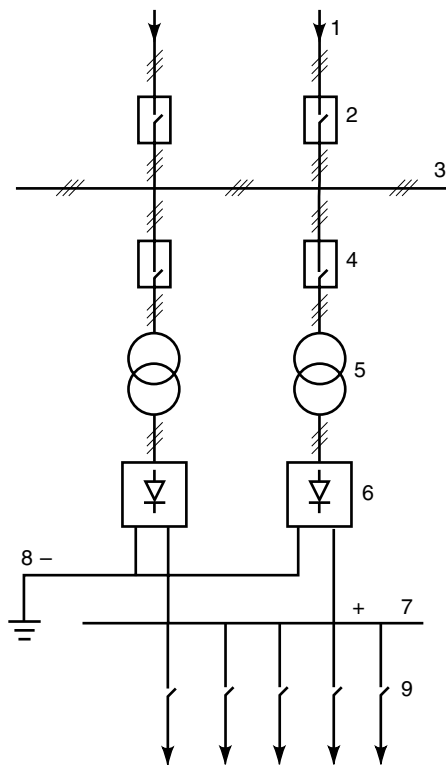


Figure 1. Basic scheme of an electrical supply substation: (1) high-voltage 3-phase lines; (2) high-voltage switchgear; (3) high-voltage 3-phase busbars; (4) primary switchgears; (5) 3-phase transformers; (6) conversions groups; (7) dc positive busbar; (8) dc negative busbar; (9) high-speed circuit breakers.

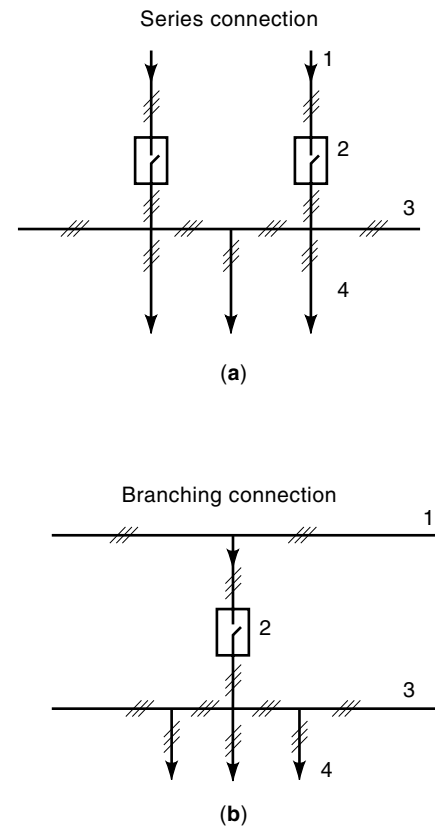


Figure 2. Series connection (a) and branching connection (b) of electrical substation to primary lines: (1) high-voltage 3-phase lines; (2) high-voltage switchgears; (3) high-voltage 3-phase busbars; (4) conversion groups supply.

connection configuration does not present any particular issue with respect to the 6-pulse. (See Appendix.)

RECTIFIER UNIT

Because of the high power involved in an electrified traction system, multiphase rectifiers are used in traction substations. Therefore, in this section a generalized analysis of a multiphase diode rectifier circuit is presented (2) (Fig. 3). All the diodes are reverse biased, and therefore nonconducting, except the one connected to the supply terminal at the highest potential with respect to the neutral. As each supply terminal in turn assumes the highest potential, the load current is transferred to the diode connected to it, and the output volt-

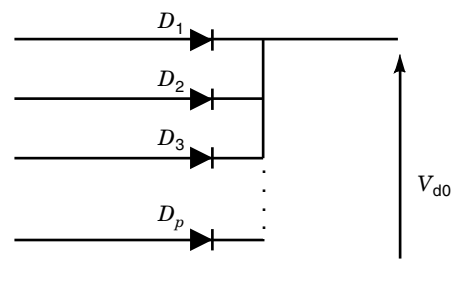


Figure 3. Multiphase diode rectifier circuit.

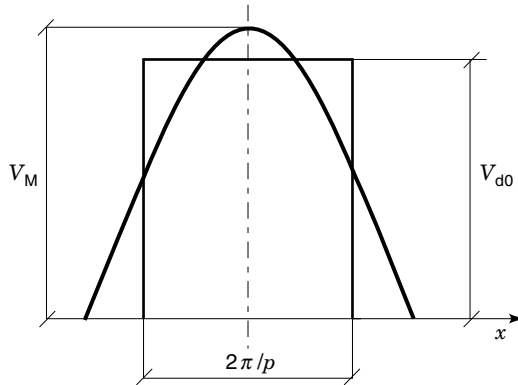


Figure 4. Calculation of V_{d0} which increases reducing conduction time $2\pi/p$.

age waveform thus consists of a sequence of parts of supply phase voltages. The current transfer from one phase to another of higher potential is known as natural commutation. In studying the behavior of a generalized rectifier unit, we make the following assumptions: resistances, inductances, and capacitances are concentrated and equal in each phase; the alternating voltages are sinusoidal and balanced; the diodes are ideal and have equal conduction time. Based on these assumptions, we can derive the general expression of the average open circuit dc voltage

$$V_{d0} = V_M \frac{p}{\pi} \sin \frac{\pi}{p} \quad (1)$$

where V_M is the peak value of the line to line voltage and p is the pulse number (number of nonsimultaneous commutations per cycle of the fundamental alternating voltage). The conduction time of each branch is then $2\pi/p$ (Fig. 4). Table 1 lists values of V_{d0}/V_M in dependence of different pulse number values: the ratio increase with increasing pulse number and with $p = 12$ its value is 0.989. The average current in each diode is

$$\bar{I}_D = \frac{I_D}{p} \quad (2)$$

where I_D is the average dc current. The root mean square (rms) current in each diode is

$$I_D = \frac{I_D}{\sqrt{p}} \quad (3)$$

whence the diode current has a form factor

$$K_f = \frac{\bar{I}_D}{I_D} = \sqrt{p} \quad (4)$$

Table 1. V_{d0}/V_M in Dependence of Pulse Number

Pulse Number	V_{d0}/V_M
2	0.637
3	0.827
6	0.955
12	0.989
∞	1

Because the ac source, especially the transformer, has inductance, the transfer of current from one phase to another requires a finite time, called commutation time or overlap time, u/ω , where u is the overlap angle and ω is the pulsation. In normal operation u is less than 60° : typical full-load values are from 20° to 25° .

A converter with pulse number p generates harmonic voltages on the dc side of orders (3)

$$h = pq \quad (5)$$

where q is any integer, and harmonic currents on the ac side of orders

$$h = pq \pm 1 \quad (6)$$

The amplitudes of harmonics decrease with increasing order: in fact, the ac harmonic current amplitude decrease of the quantity $1/k$ with respect to the amplitude of the fundamental current, whereas the dc harmonic voltage amplitude decrease of $1/k^2$. Unless measures are taken to limit the amplitude of the harmonics entering the ac network and the dc line, some of the following undesirable effects may occur: overheating of capacitors and generators, instability of converter control systems, and interference with telecommunication systems. Moreover, these effects may not be confined to the vicinity of the converter station but may be propagated over great distances. The principal means of reducing the harmonic production output of converters are to increase the pulse number and installation of filters. High pulse numbers have been used in some converters, but it is the general opinion that for high-voltage (HV) dc converters the use of filters is more economical than an increase in the pulse number beyond 12. Filters are nearly always used on the ac side of converters. Considering an ideal p -phase bridge converter (zero ac system impedance and infinite smoothing dc side inductance), the phase current consists of a periodic train of alternately positive and negative rectangular pulses of width $w = 2\pi/p$, repeating at the supply frequency. Figure 5 shows the phase current, where the broken curved lines indicate qualitatively how overlap would modify the front and tail of the current pulses. The Fourier series for the positive current pulse is

$$F_p = \frac{2}{\pi} \left(\frac{w}{4} + \sum_{m=1}^{\infty} \frac{1}{m} \sin \frac{mw}{2} \cos m\omega t \right) \quad (7)$$

which has a constant term and cosine terms of every harmonic frequency. Similarly, the Fourier series for the negative current pulse is

$$F_n = \frac{2}{\pi} \left[-\frac{w}{4} + \sum_{m=1}^{\infty} (-1)^m \frac{1}{m} \sin \frac{mw}{2} \cos m\omega t \right] \quad (8)$$

Then, the corresponding Fourier series for the train of alternately positive and negative rectangular pulses is

$$F = F_p + F_n = \frac{4}{\pi} \sum_{m=1,3,5,\dots}^{\infty} \frac{1}{m} \sin \frac{mw}{2} \cos m\omega t \quad (9)$$

where the constant term and all even harmonics have vanished. The rms magnitudes of the harmonic voltages of the dc

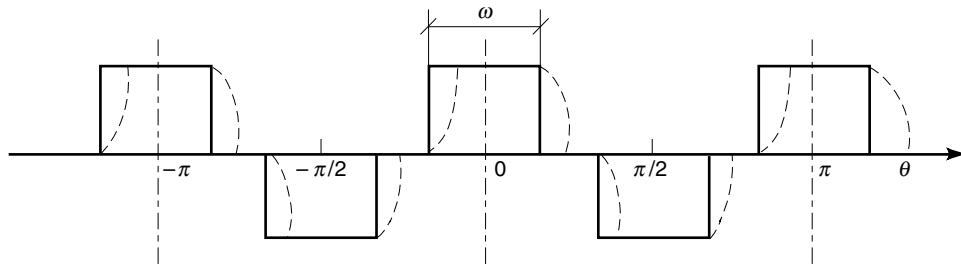


Figure 5. Trains of positive and negative rectangular pulses of arbitrary width w .

voltage waveform is

$$V_k = \frac{V_{co}}{\sqrt{2}(k^2 - 1)} \left\{ (k^2 - 1) \cos^2 \left[(k + 1) \frac{u}{2} \right] + (k^2 + 1) \cos^2 \left[(k - 1) \frac{u}{2} \right] + \left[-2(k - 1)(k + 1) \cos \left[(k + 1) \frac{u}{2} \right] \cos \left[(k - 1) \frac{u}{2} \right] \cos u \right] \right\}^{1/2} \quad (10)$$

where u is the overlap angle. If this overlap angle is zero, Eq. (10) reduces to

$$V_k = \frac{\sqrt{2}V_{co}}{k^2 - 1} \cong \frac{\sqrt{2}}{k^2} V_{co} \quad (11)$$

In practice, the ac system voltages and impedances are never perfectly balanced, therefore uncharacteristic harmonics, not considered here, can appear in the system (4) (see Fig. 6).

6-Pulse Rectifier

The basic scheme of the 6-pulse conversion unit, known in Europe as the Graetz circuit, is shown in Fig. 7(a), where the single diodes can be actually a set of series or parallel connected diodes. Moreover, dynamic and static components for voltage sharing in parallel with such diodes (resistors and $R-C$ circuits) can be considered. The rectifier can be approached by means of the definition of an equivalent star circuit (freewheeling diodes are not permitted).

According to this method, the transformer can be represented by the equivalent single phase circuit shown in Fig. 7(b), where the equivalent phase reactance X is evaluated on the basis of the short circuit tests of the transformer and is given by

$$X = \frac{V_2^2}{100A_n} V_{sc}\% \quad (12)$$

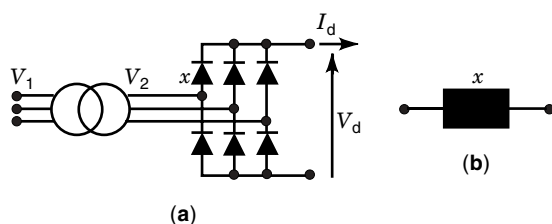


Figure 6. (a) 6-Pulse and parallel 12-pulse voltage waveform; (b) real voltage waveform including overlap angle.

where V_2 is the line to line secondary rated voltage of the transformer, A_n is the transformer rated power, and $V_{sc}\%$ is the percent short circuit voltage.

From the static point of view then, considering the features of power delivered to the traction line and load, the rectifiers are considered according to their output voltage regulation characteristic, which represents the link between the average dc voltage and the average dc output current of the rectifiers. Such characteristic is often used to assess remote short circuit current (when the fault is far enough from the dc terminals of the substation to make the overshoot current disappear, or with significant smoothing reactors at the dc terminals) and to compute average current and voltage in normal operation. According to Eq. (1) the average open-circuit dc voltage is given by

$$V_{d0} = 1.35V_2 \quad (13)$$

If the dynamic voltage sharing $R-C$ circuits in parallel with each diode in the actual configuration of the rectifier are considered as mentioned previously, then under in ideal open circuit conditions

$$V_{d0} = \sqrt{2}V_2 \quad (14)$$

but as current begins to flow into the load, the voltage rapidly decreases to the value given by Eq. (13). Referring to average dc voltage and average dc current, the 6-pulse rectifier presents three operation ranges, depending on the number of diodes which conduct simultaneously. The voltage regulation characteristic is normally evaluated neglecting the resistive voltage drop with respect to the reactive voltage drop due to overlap. In the first operational range (regular commutation with $u \leq 60^\circ$) there are no more than three diodes simultaneously conducting. The relationship between V_d and I_d in range 1 is linear and is given in Table 2. In range 2 three diodes conduct simultaneously and the relationship is elliptical. In range 3, three or four diodes conduct simultaneously and the

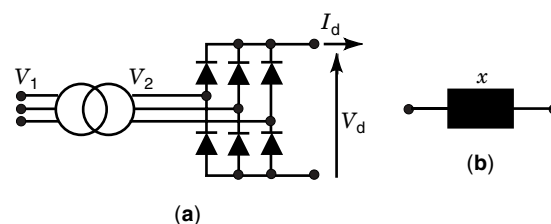


Figure 7. Reference scheme for 6-pulse rectifier unit (a); Equivalent single-phase circuit of the transformer (b).

Table 2. Relationship between V_d and I_d for 6-Pulse Rectifier

Range 1	$V_{d1} = V_{d0} - \frac{3X_c}{\pi} I_d$
Range 2	$V_{d2} = \sqrt{\frac{3}{4} \left[V_{d0}^2 - \left(\frac{6X_c}{\pi} I_d \right)^2 \right]}$
Range 3	$V_{d3} = \sqrt{3} V_{d0} - \frac{9X_c}{\pi} I_d$

relationship is linear again. The voltage regulation characteristic of the rectifier is shown in Fig. 8. The first linear region defines the equivalent resistance of the rectifier

$$R_{eq} = \frac{3X_c}{\pi} \quad (15)$$

where X_c is the commutation reactance. If $u \leq 60^\circ$, the substation can be represented by the equivalent ideal dc voltage source V_{d0} (average open circuit voltage) and by the equivalent series nonlinear resistance $R_{eq}(I_d)$, as shown in Fig. 9. Normally the conversion unit is rated in order to operate in this mode: The dc side current at the transition from range 1 to range 2 is given by

$$\frac{X_c I_{d(1 \rightarrow 2)}}{V_{d0}} = \frac{\pi}{12} \quad (16)$$

so that the calculation of the dc voltage drop according to the equivalent resistance is valid if

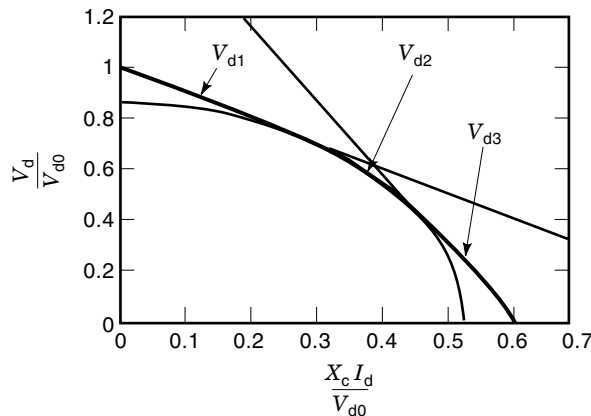
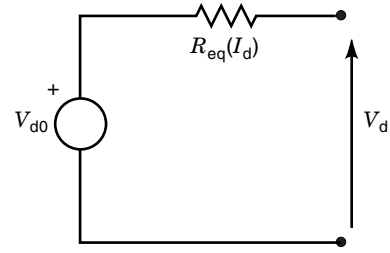
$$\frac{X_c I_d}{V_{d0}} \leq \frac{\pi}{12} \quad (17)$$

When the average dc current I_d corresponds to the secondary rated current of the transformer I_2 then $I_d = I_{rated}$, it is

$$\frac{X_c I_{d \text{ rated}}}{V_{d0}} = \frac{\pi}{6} x \quad (18)$$

where x is the per unit (p. u.) short circuit voltage for a single secondary transformer. Then

$$\frac{I_{d(1 \rightarrow 2)}}{I_{d \text{ rated}}} = \frac{1}{2x} \quad (19)$$


Figure 8. Voltage regulation characteristic of the 6-pulse rectifier.

Figure 9. Static equivalent circuit of the 6-pulse rectifier.

Assuming for example $x = 0.1$, according to Eq. (18) the current at the limit of the regular commutation range is five times the rated current of the rectifier. Maximum allowed overload current, which could be 2.5 times the rated current, is still in the regular commutation range, and the equivalent circuit in Fig. 9 is valid with R_{eq} given by Eq. (15).

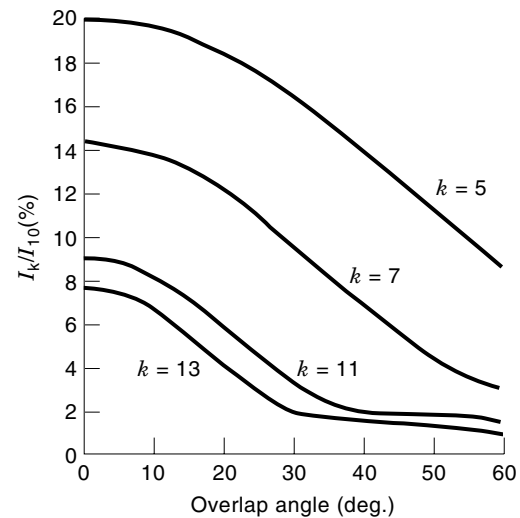
Current and Voltage Characteristic Harmonics. Substituting $\omega = 2\pi/3$ in Eq. (9) and inserting the average dc current I_d , the frequency domain expression of the ac phase current

$$i = \frac{2\sqrt{3}}{\pi} I_d \left\{ \cos \omega t + \sum_{q=1}^{\infty} \mp \frac{1}{6q \mp 1} \cos[(6q \mp 1)\omega t] \right\} \quad (20)$$

with the origin of ωt taken at the center of the positive pulse of Fig. 5. The current in the other two phases is shifted $2\pi/3$ rad and $4\pi/3$ apart. The line currents on the network side have the same waveform, hence the same harmonics, as those on the diode side if the transformer is connected star-star or delta-delta taking into account at the turns ratio. For a delta-star connection, the ac line phase current becomes

$$i = \frac{2\sqrt{3}}{\pi} I_d \left\{ \cos \omega t + \sum_{q=1}^{\infty} \pm \frac{1}{6q \pm 1} \cos[(6q \pm 1)\omega t] \right\} \quad (21)$$

The series in Eq. (20) and Eq. (21) contain only harmonics of order $6q \pm 1$, according to Eq. (6). Figure 10 shows the magnitude of the fifth, seventh, eleventh, and thirteenth current harmonics related to the fundamental component as functions of the overlap angle for a 6-pulse converter. Figure 11 shows


Figure 10. Fifth, seventh, eleventh, and thirteenth current harmonics of a 6-pulse converter.

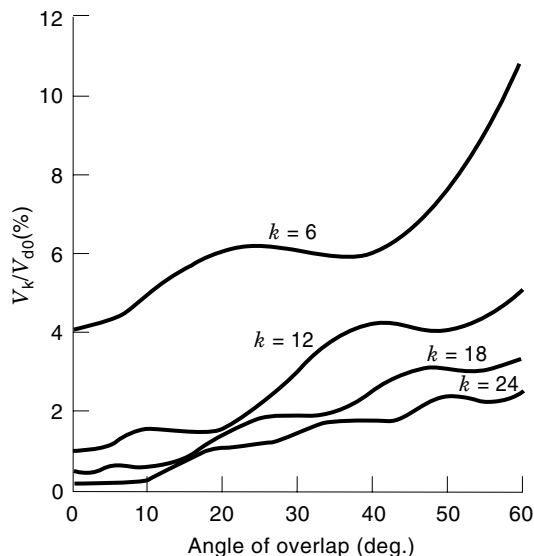


Figure 11. Sixth, twelfth, eighteenth, and twenty-fourth harmonic of direct voltage of a 6-pulse converter.

the magnitude of the sixth, twelfth, eighteenth, and twenty-fourth voltage harmonics as a percentage of the fundamental component as functions of the overlap angles for a 6-pulse converter.

12-Pulse Rectifier

Figure 12(a) shows the 12-pulse unit in the parallel configuration, the most frequent in electric traction applications. The transformer can be represented by the equivalent single

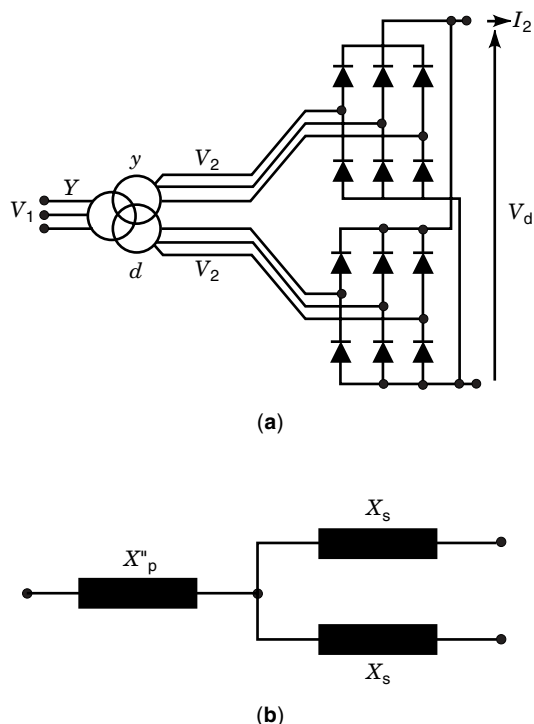


Figure 12. Reference scheme for 12-pulse rectifier unit (a); Equivalent single-phase circuit of the transformer (b).

phase circuit shown in Fig. 12(b), where the secondary reactances X_s are assumed to be equal. Normally they are not equal, because of constructive differences and approximate realization of the ratio between the turns ratios of the delta and wye secondary windings, which should equal $\sqrt{3}$, and is based on rational ratios such as 11/19, 15/26, and so on. On multiple winding transformer tests, the recommendations prescribe that each short circuited winding, one supplied with the test voltage, and the others open circuit [case (1), binary tests]. Sometimes for three winding transformer tests the secondary windings are short circuited together and the global short circuit voltage is measured [case (2)]. In case (1) the reactances are given by the following formulas

$$X_p'' = \frac{V_2^2}{100A_n} (2V_{sc12}\% - V_{sc23}\%); X_s = \frac{V_2^2}{100A_n} V_{sc23}\% \quad (22)$$

where V_{sc12} is the primary to secondary 2 short circuit voltage with secondary 3 open circuit, V_{sc23} is the primary to secondary 3 short circuit voltage with secondary 2 open circuit and A_n is the transformer rated power. In case (2) it is

$$X_p'' = \frac{2V_2^2}{100A_n} (V_{sc1(23)}\% - V_{sc12}\%); \quad (23)$$

$$X_s = \frac{2V_2^2}{100A_n} (2V_{sc12}\% - V_{sc1(23)}\%)$$

where $V_{sc1(23)}$ is the primary to parallel connected secondaries short circuit voltage. It has to be noted that V_{sc12} is supposed to be equal to V_{sc13} where V_{sc13} is the primary to secondary 3 short circuit voltage with the secondary 2 open circuit (on the basis of the assumption made on X_s) and both are measured on $A_n/2$ base power, and so is V_{sc23} , while $V_{sc1(23)}$ is measured on A_n base power. Resistances are normally available in test reports from dc measurements or short circuit loss measurements. If needed, more accuracy can be achieved by exact computation of reactances.

The most significant parameter for the analysis of the static behavior of the 12-pulse rectifier is the coupling factor (or reactance ratio) k , defined by the following equation

$$k = \frac{X_p}{X_s + X_p} = \frac{X_p''}{X_s + X_p''} \quad (24)$$

where X_p'' is the primary reactance seen from the secondary, X_s' is the secondary reactance seen from the primary, X_s is the secondary reactance, and $X_p'' + X_s = X_c$ is the commutation reactance. Ideally the coupling factor value can change from 0 (reactance concentrated at the secondary windings) to 1 (reactance concentrated at the primary winding). The case with $k = 0$ is equivalent to two six-pulse rectifier units in parallel on the dc side with independent transformers. The circuit in Fig. 9 is then modified according to the dependence of the average dc voltage on the value of the coupling factor as shown in Fig. 13. According to Eq. (1) the average open circuit dc voltage is given by

$$V_{d0} = 1.398V_2 \quad (25)$$

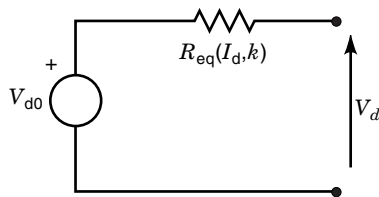


Figure 13. Static equivalent circuit of the 12-pulse rectifier.

Similarly to the 6-pulse rectifier, if we consider the above dynamic voltage sharing R - C circuits which are parallel with each diode in the actual configuration of the rectifier, then in ideal open circuit conditions

$$V_{d0} = \sqrt{2}V_2 \quad (26)$$

but as current begins to flow into the load, the voltage rapidly decreases to the value given by Eq. (25). Actually, during load operation the dc voltage corresponds to the average value of the dc voltages produced by the single bridges, which is given by Eq. (13). It is possible to have a configuration of the 12-pulse rectifier with an intergroup reactor (Fig. 14). In this case, a center-tapped inductor is placed between the two rectifier groups and is usually connected to the neutral and to the negative pole of the dc line. When the average dc current I_d reaches the value I^* (shown in the enlarged detail of Fig. 15) at the end of the intermittent conduction range of the two bridges (depending on the effect of the secondary reactances of the transformer and the intergroup reactor, if present) the characteristic can be considered correspond to the average open circuit dc voltage given by Eq. (13). It has to be considered that the presence of the intergroup reactor has no effect on the assumptions made in this article. Being the correct sharing of the dc current among the two 6-pulse bridges of the 12-pulse unit guaranteed by the secondary reactances of the transformer only, which should be equal, the intergroup reactor has no other feature than supporting the instantaneous voltage difference between the two bridges and reducing the circulation current to specified value. The intergroup reactor has no dynamic effects on the output dc current: the only smoothing effect on the dc current can be associated to the leakage inductance due to the imperfect coupling between the two parts of the winding of the reactor. Such effect could

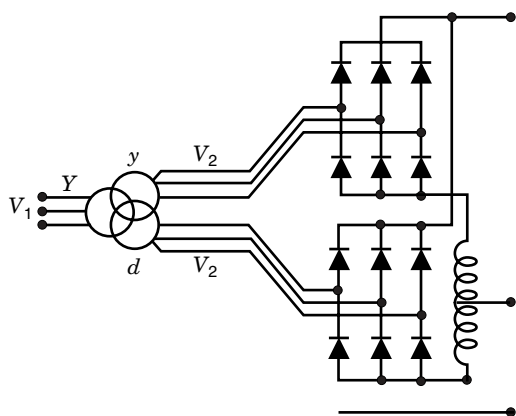


Figure 14. Twelve-pulse rectifier with intergroup reactor.

be requested as an additional feature of the reactor to achieve a compact intergroup reactor-smoothing reactor-capacitor assembly for the line low pass filter, but this case is not considered here. An ideal intergroup reactor has no effects on steady state and transient dc short circuit current.

The value of the coupling factor is normally required of the manufacturer in order to control the voltage regulation characteristic of the conversion unit: the effect of the variation of k from 0 to 1 is shown in Fig. 15. It can be seen how the short circuit current with the same slope in the initial linear range can differ. Usually k is required to be as near to unity as possible in metrorail plants, where short circuit currents must be limited to reasonable values, because of the short distance between substations and the high-rated power of rectifiers with low-rated voltage. In railway plants short circuit currents must be recognized from overloads or transient overcurrents, which can present the same order of magnitude because of the longer distance between substations and of the higher rated voltage (e.g., 3 kV). On the basis of the available data on the test report of the transformer, the coupling factor can be immediately evaluated. For case (1) it results in

$$k = 1 - \frac{x_{23}}{2x_{12}} \quad (27)$$

where x_{23} is the secondary 2 to the secondary 3 p. u. short circuit voltage with the primary open circuit, and x_{12} is the primary to secondary 2 p. u. short circuit voltage with secondary 3 open circuit. And in case (2)

$$k = \frac{x_{1(23)}}{x_{12}} - 1 \quad (28)$$

where $x_{1(23)}$ is the primary to parallel connected secondaries p. u. short circuit voltage. On the basis of the coupling factor, of the commutation reactance and of the no-load average dc voltage of the conversion unit, the steady-state voltage regulation characteristic can be evaluated. The direct output current I_d is supposed to be perfectly smoothed and the resistances of the transformer windings are neglected. These two fundamental assumptions allow the analytical resolution of the equations (5). If the coupling factor varies in the following range

$$0 < k < \frac{\sqrt{3} - 1}{\sqrt{3}} \quad (29)$$

the voltage regulation characteristic presents five operation ranges (with the last one divided into two subranges). If

$$\frac{\sqrt{3} - 1}{\sqrt{3}} < k < \frac{2}{3} \quad (30)$$

then the second subrange of the fifth range does not exist. If

$$\frac{2}{3} < k < 1 \quad (31)$$

then the fifth range does not exist. Table 3 lists the voltage regulation characteristic V_d - I_d relationship. Figure 16 shows

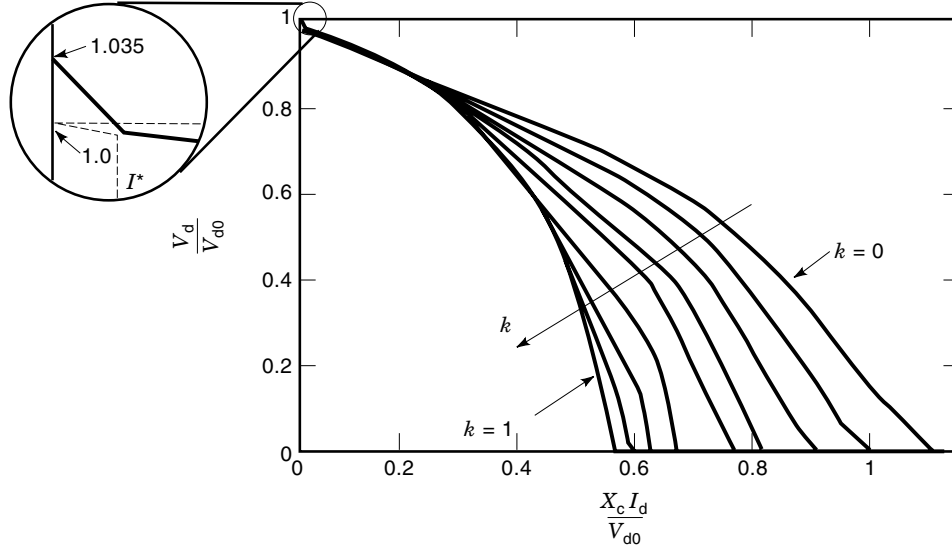


Figure 15. Variation of the voltage regulation characteristic of the 12-pulse rectifier as a function of the coupling factor k .

the complete voltage regulation characteristic of the 12-pulse rectifier, together with its components in each operation range, for $k = 0.13$, typical of standard transformers used by the Italian Railways. The linear behavior of the characteristic in range 1 leads to the definition of the equivalent output resistance of the conversion unit

$$R_{\text{eq}} = \frac{3X_c}{2\pi} \quad (32)$$

which allows one to evaluate the direct voltage drop in range 1. Normally the dc rated current value is chosen within range 1: the dc current at the transition from range 1 to range 2 is not a function of k and is given by

$$\frac{X_c I_d}{V_{d0}} = \frac{\pi(2 - \sqrt{3})}{6} \quad (33)$$

When the average dc current I_d corresponds to the secondary rated current of the transformer I_2 then $I_d = I_{d \text{ rated}}$, and

$$\frac{X_c I_{d \text{ rated}}}{V_{d0}} = \frac{\pi}{3} x_{12} \quad (34)$$

then

$$\frac{I_{d(1 \rightarrow 2)}}{I_{d \text{ rated}}} = \frac{2 - \sqrt{3}}{2x_{12}} \quad (35)$$

Assuming for example $x_{12} = 0.1$, according to Eq. (35) the current at the limit of the regular commutation range is only 1.34 times the rated current of the rectifier. Maximum allowed overload current, which could be 2.5 times the rated current, is out of the regular commutation range. The voltage regulation characteristic degenerates if $k \rightarrow 0$ and if $k \rightarrow 1$. If $k \rightarrow 0$ range 2 does not exist any more, and range 1 and 3 are joined together in a single straight line with slope $-3X_c/2\pi$ (as can be verified by substituting $k = 0$ in the equation of range 3). Range 4 collapses to the elliptical curve given by the equation corresponding to the second range of the 6-pulse rectifier with $X_c/2$. Subranges 1 and 2 of range 5 give the same straight line (as can be verified by substituting $k = 0$ in the equations corresponding to the third range of the 6-pulse rectifier with $X_c/2$). The case when $k = 0$ is then equivalent to two independent transformers, as stated before. If $k \rightarrow 1$ range 4 and range 5 disappear, and range 3 is given by the

Table 3. Relationship between V_d and I_d for 12-Pulse Rectifier

Range 1	$V_{d1} = V_{d0} - \frac{3X_c}{2\pi} I_d$
Range 2	$V_{d2} = \frac{\sqrt{2}(\sqrt{3} + 1)}{4} \sqrt{V_{d0}^2 - \frac{1}{2 - \sqrt{3}} \left(\frac{3}{\pi} X_c I_d \right)^2}$
Range 3	$V_{d3} = \frac{\sqrt{3}(1 - k)^2 + 1}{2 - \sqrt{3}k} V_{d0} - \frac{3}{2\pi} \frac{2 + \sqrt{3}k}{2 - \sqrt{3}k} X_c I_d$
Range 4	$V_{d4} = \frac{\sqrt{3}(1 - k)}{2 - \sqrt{3}k} \sqrt{V_{d0}^2 - (2 + \sqrt{3}k)^2 \left(\frac{3}{2\pi} X_c I_d \right)^2}$
Range 5.1	$V_{d5.1} = \frac{\sqrt{3}(1 - k)(8 - 3k^2)}{2(2 - \sqrt{3}k)\sqrt{3(1 - k)^2 + 1}} V_{d0} - \frac{9}{2\pi} \frac{(1 - k^2)(2 + \sqrt{3}k)}{2 - \sqrt{3}k} X_c I_d$
Range 5.2	$V_{d5.2} = \frac{\sqrt{3}(1 - k)(4 - 3k)}{2\sqrt{3(1 - k)^2 + 1}} V_{d0} - \frac{9}{2\pi} (1 - k^2) X_c I_d$

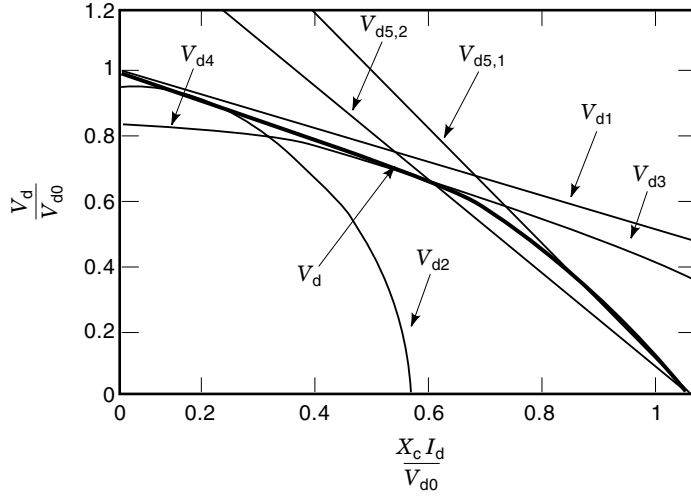


Figure 16. Voltage regulation characteristic of the 12-pulse rectifier ($k = 0.13$).

straight line

$$V_{d3} = (2 + \sqrt{3})V_{d0} - (2 + \sqrt{3})^2 \frac{3X_c I_d}{2\pi} \quad (36)$$

Current and Voltage Characteristic Harmonics

Since the 12-pulse rectifier consists of two 6-pulse groups fed from two sets of 3-phase transformers in parallel, with their fundamental voltage equal and phase-shifted by $\pi/6$, the resultant network side current of the two groups is given by the sum of Eq. (20) and Eq. (21)

$$i = \frac{4\sqrt{3}}{\pi} I_d \left\{ \cos \omega t + \sum_{q=1}^{\infty} \mp \frac{1}{12q \mp 1} \cos[(12q \mp 1)\omega t] \right\} \quad (37)$$

which contains only harmonics of order $12q \pm 1$, according to Eq. (6). The harmonic currents of order $6q \pm 1$ (with q odd) circulate between the two converter transformers but do not penetrate the ac network. Figure 17 shows the magnitude of

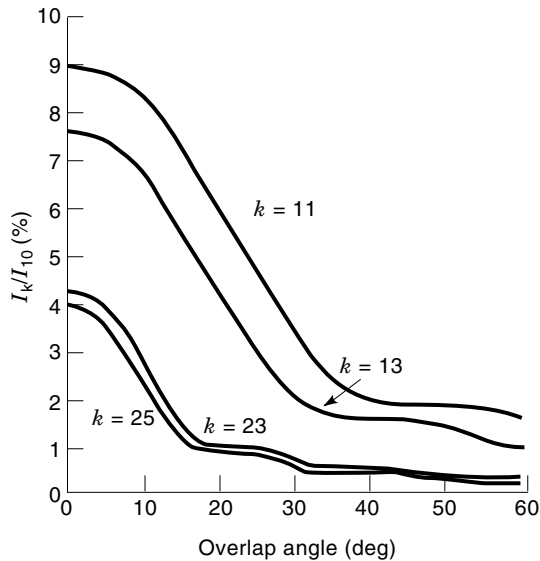


Figure 17. Eleventh, thirteenth, twenty-third, and twenty-fifth current harmonics of a 12-pulse converter.

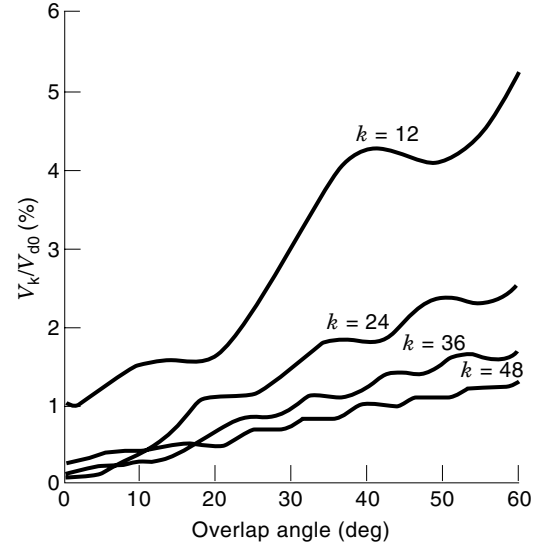


Figure 18. Twelfth, twenty-fourth, thirty-sixth, and forty-eighth harmonic of direct voltage of a 12-pulse converter.

the eleventh, thirteenth, twenty-third, and twenty-fifth current harmonics related to the fundamental component in terms of overlap angles for a 12-pulse converter. Figure 18 shows the magnitude of the twelfth, twenty-fourth, thirty-sixth, and forty-eighth voltage harmonics as a percentage of the fundamental component in terms of overlap angles for a 12-pulse converter.

SHORT CIRCUIT FOR ZERO FAULT IMPEDANCE CURRENTS

Short Circuit Current for 6-Pulse Rectifier

The steady-state short circuit current is given by

$$\frac{X_c I_{sc0}}{V_{d0}} = \frac{\pi\sqrt{3}}{9} \quad (38)$$

The transient short circuit current at zero fault impedance and a more accurate value of the steady-state average short circuit current can be evaluated if we remove the assumption of perfectly smoothed direct current and negligible windings resistances. To this aim, the equivalent star circuit of the converter is considered. The short circuit equivalent impedance is given by

$$Z_{sc} = (R_p'' + R_s) + j\omega(L_p'' + L_s) = R_c + j\omega L_c = Z_c \quad (39)$$

where R_p'' is the primary resistance seen from the secondary, R_s is the secondary resistance, L_p'' is the primary inductance seen from the secondary, L_s is the secondary inductance, R_c is the commutation resistance, L_c is the commutation inductance, and Z_c is the commutation impedance. The short circuit equivalent time constant is defined by

$$\tau_{sc} = \tau_c = \frac{L_c}{R_c} \quad (40)$$

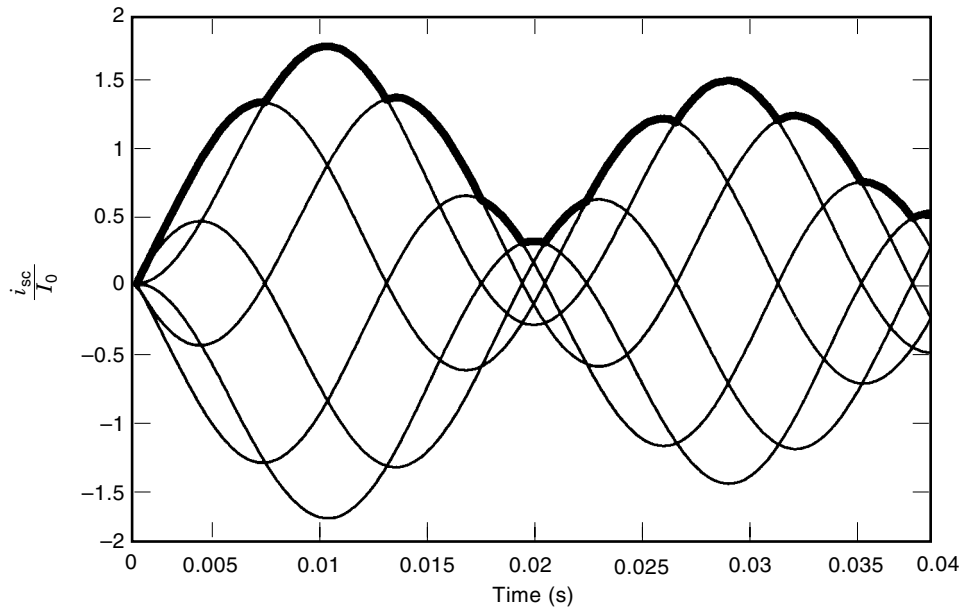


Figure 19. Transient short circuit current in the 6-pulse bridge.

The amplitude of the steady-state equivalent phase short circuit at zero fault impedance is given by

$$I_0 = \frac{\sqrt{2}E}{\sqrt{R_c^2 + \omega^2 L_c^2}} \quad (41)$$

where E is the rms phase voltage. The transient short circuit current in the j th phase of the star equivalent circuit is (6)

$$i_{scj}(t) = I_0 [\cos(\omega t + \varphi_j - \varphi_c) - \exp(-t/\tau_{sc}) \cos(\varphi_j - \varphi_c)] \quad (42)$$

where: $\varphi_{sc} = \text{atan}(\omega L_c / R_c) = \text{atan } \omega \tau_c$, φ_j is the voltage phase shift with respect to the common phase reference, and φ_c is the commutation impedance phase angle. Figure 19 shows the transient dc side short circuit current which is given by the envelope of the maximum values of the currents of the j phases. This leads to the evaluation of the accurate value of the steady-state short circuit current

$$I_{sc0} = \frac{3}{\pi} I_0 = \frac{3}{\pi} \frac{\sqrt{2}E}{\sqrt{R_c^2 + X_c^2}} = \frac{V_{d0}}{\sqrt{3}\sqrt{R_c^2 + X_c^2}} \quad (43)$$

Figure 20 shows the circuit represented in Fig. 8 at short circuit conditions, where the equivalent short circuit resistance is given by

$$R_{eqsc} = \sqrt{3}\sqrt{R_c^2 + X_c^2} = \sqrt{3}Z_{sc} = \sqrt{3}Z_c \quad (44)$$

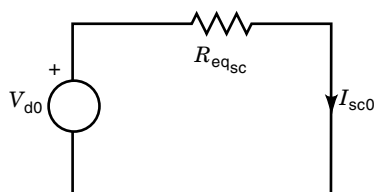


Figure 20. Equivalent circuit at steady-state short circuit conditions.

One of the equivalent currents in Fig. 19 gives the peak value of the short circuit current, which depends on the instant at which the fault occurs. Assuming that the fault occurs at $t = 0$, the worst case in terms of peak is verified for $\varphi_j = -3\pi/2$, and the expression for the transient current presenting the first and higher peaks (and the following ones) is

$$i_p(t) = I_0 [\sin(\omega t - \varphi_c) + \exp(-t/\tau_c) \sin(\varphi_c)] \quad (45)$$

Figure 21 shows the phase current corresponding to the peak dc transient short circuit. The expression of the approximate instantaneous dc short circuit current wave form can be written as

$$i_{sca}(t) = I_{p0} [1 + \exp(-t/\tau_c) \sin(\omega t - \varphi_c)] \quad (46)$$

where $I_{p0} = I_0$.

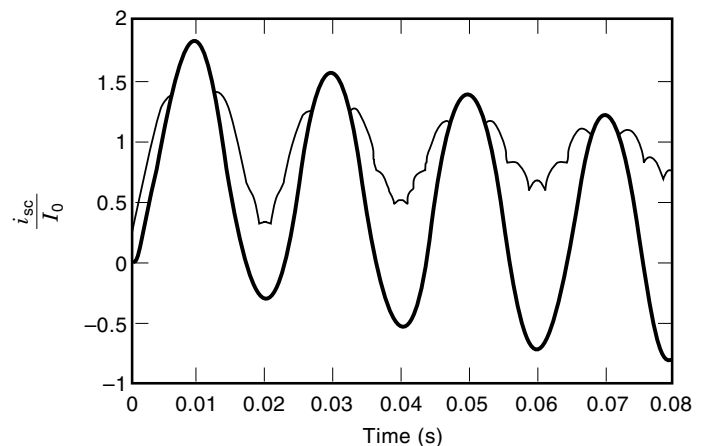


Figure 21. Phase current corresponding to the peak dc short circuit current for the 6-pulse bridge. (Bold line curve: phase current corresponding to the peak short circuit current for 6-pulse bridge. Thin line curve: short circuit current.)

Short Circuit Current for 12-Pulse Rectifier

In the 12-pulse rectifier, for a fixed value of the commutation reactance X_c the zero-impedance steady-state short circuit current can take different values depending on the coupling factor k [Eq. (24)] (7). If

$$0 < k < \frac{\sqrt{3}-1}{\sqrt{3}} \quad (47)$$

the steady-state short circuit current can be evaluated according to the following relationship

$$\frac{X_c I_{sc0}}{V_{d0}} = \frac{\sqrt{3}(4-3k)\pi}{9(1-k)\sqrt{3}(1-k^2)+1} \quad (48)$$

If

$$\frac{\sqrt{3}-1}{\sqrt{3}} < k < \frac{2}{3} \quad (49)$$

then

$$\frac{X_c I_{sc0}}{V_{d0}} = \frac{\sqrt{3}(8-\sqrt{3}k^2)\pi}{9(1+k)(2+\sqrt{3}k)\sqrt{3}(1-k^2)+1} \quad (50)$$

If

$$\frac{2}{3} < k < 1 \quad (51)$$

then

$$\frac{X_c I_{sc0}}{V_{d0}} = \frac{2\pi}{3(2+\sqrt{3}k)} \quad (52)$$

A very good approximation of the steady-state short circuit current as a function of k is given by the following formula, for any value of k ($0 < k < 1$)

$$\frac{X_c I_{sc0}}{V_{d0}} = 0.47k^2 - 1.1k + 1.2 \quad (53)$$

so that the short circuit current can be

$$0.57 \frac{V_{d0}}{X_c} < I_{sc} < 1.2 \frac{V_{d0}}{X_c} \quad (54)$$

The steady-state short circuit current with $k \rightarrow 0$ is more than twice the current with $k \rightarrow 1$. However, it will be shown further on how the steady-state short circuit current can be calculated with more accuracy. Similarly to the 6-pulse bridge, removing the two assumptions of perfectly smoothed direct current and negligible windings resistances, the transient short circuit current at zero-fault impedance and a more accurate value of the steady-state average short circuit current can be evaluated. For the 12-pulse rectifier, the short circuit equivalent impedance is given by

$$\begin{aligned} Z_{sc} &= (2R_p'' + R_s) + j\omega(2L_p'' + L_s) \\ &= (1+k_R)R_c + j\omega(1+k_L)L_c = Z_c \end{aligned} \quad (55)$$

where k_R is the resistance ratio, simply defined analogously with the coupling factor by:

$$k_R = \frac{R_p}{R_s + R_p} = \frac{R_p''}{R_s + R_p''} \quad (56)$$

and the short circuit equivalent time constant is defined as

$$\tau_{sc} = \frac{(1+k_L)L_c}{(1+k_R)R_c} = \frac{(1+k_L)}{(1+k_R)}\tau_c \quad (57)$$

The transient short circuit current in the j th phase of the star equivalent circuit is again given by Eq. (42) in which

$$\varphi_{sc} = \text{atan} \left[\frac{\omega(1+k_L)L_c}{(1+k_R)R_c} \right] = \text{atan} \omega\tau_{sc} \quad (58)$$

and the amplitude of the steady-state equivalent phase short circuit current at zero-fault impedance is

$$I_0 = \frac{\sqrt{2}E}{\sqrt{(1+k_R)^2 R_c^2 + \omega^2 (1+k_L)^2 L_c^2}} \quad (59)$$

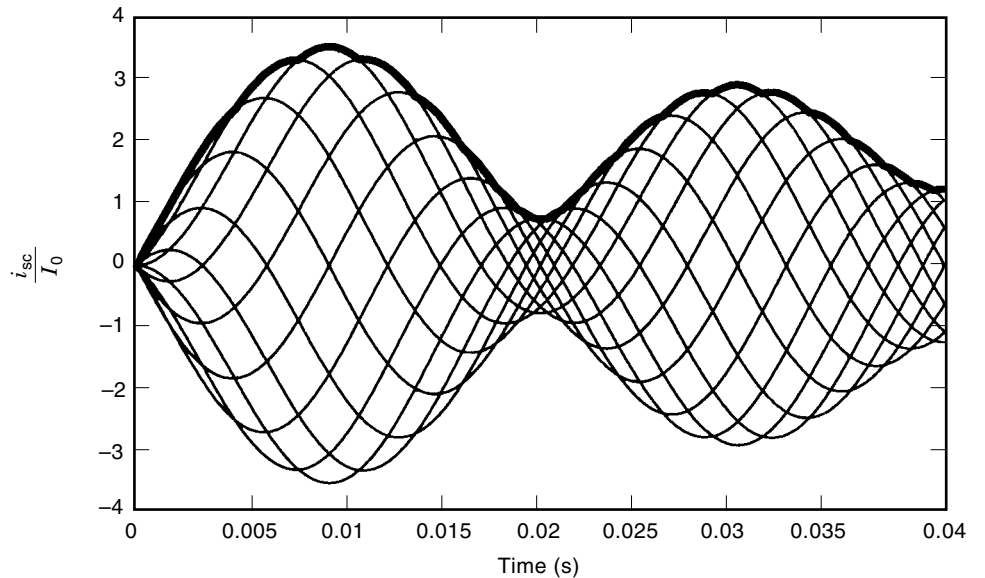


Figure 22. Transient short circuit currents in the 12-pulse rectifier.

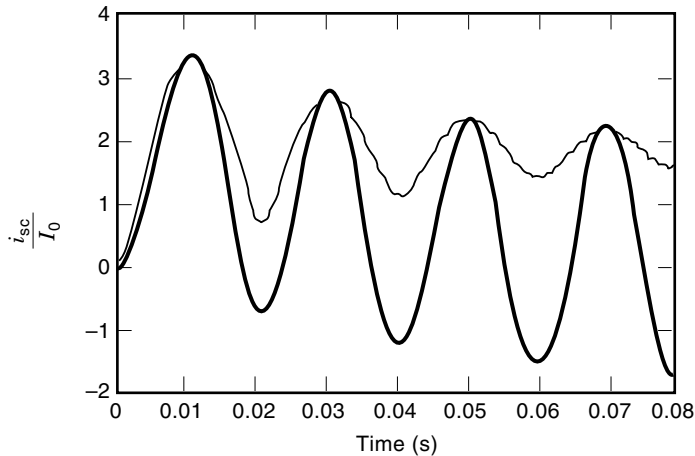


Figure 23. Phase current corresponding to the peak dc short circuit current for the 12-pulse bridge (steady state). (Bold line curve: phase current corresponding to the peak short circuit current for the 12-pulse bridge (steady state). Thin line curve: short circuit current.)

It can be assumed that $k_R = k_L = k$: the validity of the approximation depends on the particular transformer, but introduces small errors as long as resistance is small with respect to reactance. Figure 22 shows the transient dc side short circuit current which is given by the envelope of the short circuit currents of the equivalent star circuit added two by two. A more accurate value of the steady-state short circuit current is given by

$$I_{sc0} = \frac{6}{\pi} I_0 = \frac{6}{\pi} \frac{\sqrt{2}E}{(1+k)\sqrt{R_c^2 + X_c^2}} = \frac{2V_{d0}}{(1+k)\sqrt{3}\sqrt{R_c^2 + X_c^2}} \quad (60)$$

At short circuit conditions the circuit of Fig. 20 can be considered again, where the equivalent short circuit resistance values

$$R_{eq_{sc}} = \sqrt{3} \frac{1+k}{2} \sqrt{R_c^2 + X_c^2} = \frac{\sqrt{3}}{2} Z_{sc} = \frac{\sqrt{3}}{2} (1+k) Z_c \quad (61)$$

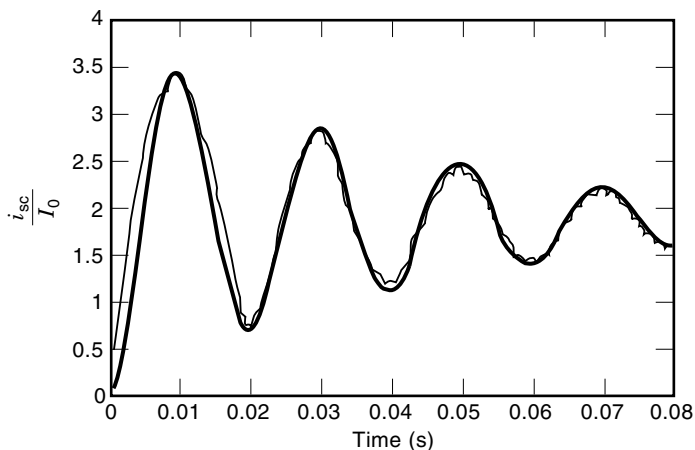


Figure 24. Approximate and real dc short circuit in the 12-pulse rectifier. [Approximate (thin line curve) and real (bold line curve) short circuit in the 12-pulse rectifier.]

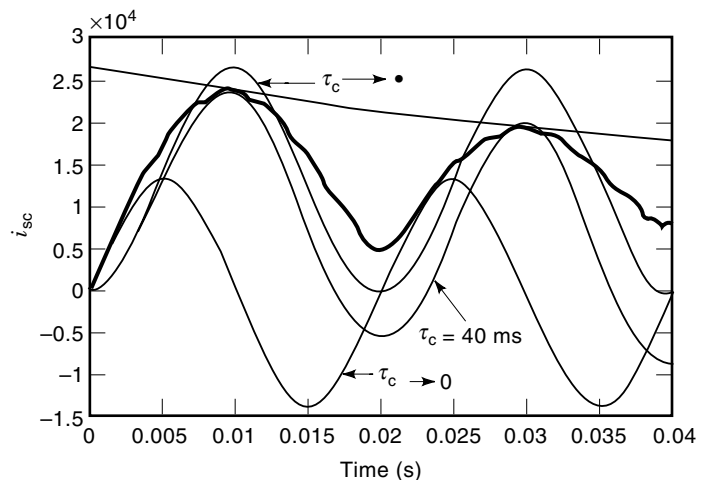


Figure 25. Limit conditions and the case with $\tau_c = 40$ ms of the short circuit current.

The worst case, which is given by $i_{12} + i_{11}$, with $\varphi_{12} = -\pi/4$, is considered in order to individualize the equivalent current in Fig. 23 that gives the peak value of the short circuit current

$$i_p(t) = \frac{1+\sqrt{3}}{\sqrt{2}} I_0 [1 + \exp(-t/\tau_c)] \sin(\omega t - \varphi_c) \quad (62)$$

The expression for the approximate short circuit current of Eq. (46) is again valid, and is

$$I_{p0} = \frac{1+\sqrt{3}}{\sqrt{2}} I_0 \quad (63)$$

for the 12-pulse rectifier.

Figure 24 shows this approximate short circuit current superimposed on the corresponding real 12-pulse dc short circuit current.

Deriving the expression of the current in Eq. (62) with respect to time and setting the derivative zero in the time inter-

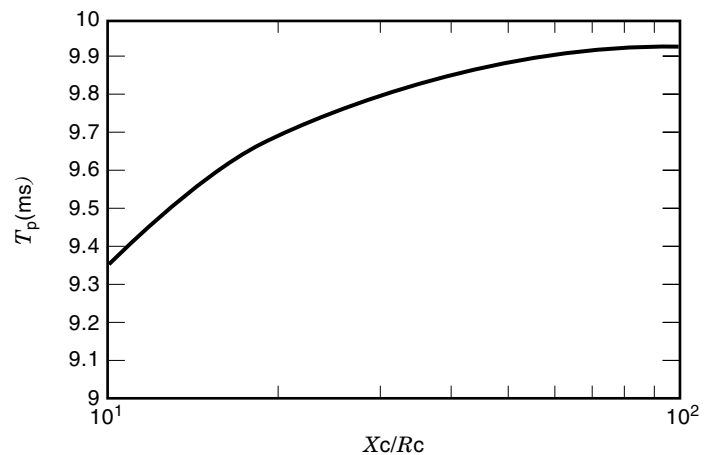


Figure 26. Current peak time as a function of the ratio X_c/R_c .

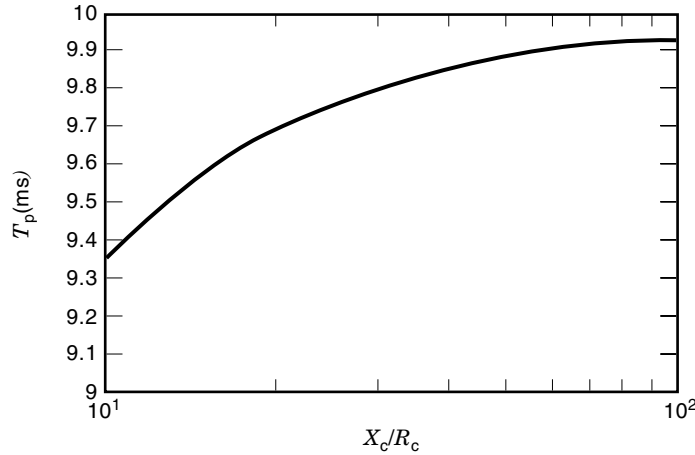


Figure 27. Current peak value as a function of the ratio X_c/R_c .

val during which the peak can occur, it is possible to find the instant at which the peak occurs

$$t_p = 2\varphi_c/\omega \tag{64}$$

and then the peak current value

$$I_{pm} = I_{p0} \left[1 + \exp\left(\frac{-2\varphi_c}{\omega\tau_c}\right) \sin\varphi_c \right] \tag{65}$$

It is obviously easy to verify that for $\tau_c \rightarrow \infty$ ($R_c = 0$, $\varphi_c = \pi/2$, $t_p = \pi/\omega$) it is $I_{pm} = 2I_{p0}$, while for $\tau_c \rightarrow 0$ ($X_c = 0$, $\varphi_c = 0$, $t_p = \pi/2\omega$) it is $I_{pm} = I_{p0}$. The limit conditions and the case with $\tau_c = 40$ ms are shown in Fig. 25, together with the exponential peaks envelope, whose expression is

$$i_e(t) = I_{p0}[\exp(-t/\tau_c) + 1] \tag{66}$$

Figure 26 shows the peak time plotted as a function of the ratio X_c/R_c which is related to the short circuit power factor of the transformer, and Figure 27 shows the value even plotted as a function of the ratio X_c/R_c .

APPENDIX

Table A contains the name plate data of a typical three-phase transformer used in a railway traction rectifier substation.

Table A

Data	Primary (1)	Secondary (2)	Secondary (3)
Rated power (MVA)	5.75	2.875	2.875
Rated voltage (kV)	150	2.710	2.710
<i>Group Yyd</i>			
$V_{sc1(23)}\%$	12.00	Short circuit voltage (primary to parallel connected secondaries)	
$V_{sc12}\%$	10.73	Short circuit voltage (primary to secondary 2, with secondary 3 open circuit)	
$V_{sc13}\%$	10.58	Short circuit voltage (primary to secondary 3, with secondary 2 open circuit)	

Table B contains the name plate data of a typical three-phase transformer used in a metrorail traction rectifier substation.

Table B

Data	Primary (1)	Secondary (2)	Secondary (3)
Rated power (MVA)	5.75	2.875	2.875
Rated voltage (kV)	150	2.710	2.710
<i>Group Yyd</i>			
$V_{sc1(23)}\%$	15.79	Short circuit voltage (primary to parallel connected secondaries)	
$V_{sc12}\%$	8.43	Short circuit voltage (primary to secondary 2, with secondary 3 open circuit)	
$V_{sc13}\%$	8.32	Short circuit voltage (primary to secondary 3, with secondary 2 open circuit)	
$V_{sc23}\%$	1.85	Short circuit voltage (secondary 2 to secondary 3, with primary open circuit)	

BIBLIOGRAPHY

1. L. Mayer, *Impianti Ferroviari*, 2nd ed. Rome: CIFI, 1993.
2. S. Crepaz, *Conversione Statica dell'Energia Elettrica*, CLUP, 1981.
3. E. W. Kimbark, *Direct Current Transmission*, vol. I, New York: Wiley, 1987.
4. J. Arillaga, D. A. Bradley, and P. S. Bodger, *Power systems harmonics*, New York: Wiley, 1985.
5. A. Del Bebbio and B. Lenzi, Caratteristiche funzionali del raddrizzatore in collegamento a ponte trifase doppio, alimentato da un trasformatore anodico con due avvolgimenti secondari sfasati di 30° elettrici, per qualunque rapporto di reattanza dispersa fra il primario ed i due secondari, *Rassegna tecnica AEG—Telefunken*, 6: 2-3, 1976.
6. L. R. Denning, Influence of commutating reactance on the design of dc power supply converters, *Power Eng. J.*, 4: 1987.
7. L. R. Denning, The effect of dc faults on substation design, *APTA Rapid Transit Conference*, 1982.

PATRIZIA FERRARI
 PAOLO POZZOBON
 Università degli Studi di Genova